Quantum well states of *sp*- and *d*-character in thin Au overlayers on W(110)

A. M. Shikin,[1,2] O. Rader,[1] G. V. Prudnikova,[2] V. K. Adamchuk,[2] and W. Gudat[1]

[1]*BESSY, Albert-Einstein-Str. 15, D-12489 Berlin, Germany*
[2]*St. Petersburg State University, St. Petersburg, 198904 Russia*

Photoemission spectra are reported for Au on W(110) which show series of pronounced peaks up to large film thicknesses [about 15 monolayer (ML)] which are assigned to quantum-well states of Au *sp* and Au *d* character. Due to its large 5*d* bandwidth and low binding energy, *sp* and *d* states are largely degenerate in Au. Therefore, Au overlayers serve as an interesting test system for simple models of quantum-well-state formation. A good description of all of the observed features is reached based on our extended phase accumulation model analysis. Assignment to several branches of *sp*- and *d*-type quantum-well states is reached based on (i) our model treatment, (ii) the asymptotic behavior for large thicknesses, (iii) an analysis of the angle dispersion, and (iv) a comparison between the system without and with an extra Ag interlayer. For the latter it is found that *sp*-type quantum-well states form throughout the combined (Au+Ag) layer already from lowest coverages on, whereas formation of *d*-type quantum-well states is largely suppressed. Using our model treatment we reach a thorough description of both systems for the whole thickness range starting out from submonolayer coverages and correct previous assignments in the literature. In addition, the role of *sp*-*d* hybridization in the overlayer is discussed.

I. INTRODUCTION

Multilayer structures composed of alternating ferromagnetic and nonmagnetic metals have recently attracted significant interest due to their intriguing properties,[1–11] most notably long-range oscillatory magnetic coupling and giant magnetoresistance.[1–3] It has been shown that the exchange coupling between magnetic layers in such systems can be alternated from ferromagnetic to antiferromagnetic and vice versa by increasing the thickness of the nonmagnetic interlayer. It has been established that such oscillatory magnetic coupling is tightly connected to the formation of quantized electronic states inside of this nonmagnetic interlayer which are the mediators of the magnetic coupling between the ferromagnetic layers.[4–6]

The materials most often used as nonmagnetic interlayers in multilayer structures are the noble metals Cu, Ag, and Au.[1–11] Their electronic structure and Fermi surface are much simpler as compared to those of, e.g., transition metals. For these reasons, the formation of quantum-well states (QWS's) formed in noble-metal layers, and their dependence on layer thickness and on the choice of the substrate, have increasingly attracted researchers' interest.[12–31]

The present work is devoted to quantum-size effects developed in ultrathin Au layers with thicknesses beginning from submonolayer coverages up to 15 ML and aims at describing the behavior of the observed QWS's in the whole valence-band range and for all Au thicknesses investigated. In contrast to Cu and Ag, for which a substantial number of QWS studies exists,[12–27] there were only a few reports devoted to Au films[27,29] despite the fact that multilayer systems fabricated on the basis of Au interlayers have shown oscillatory magnetic coupling.[7–11] Possibly this is connected to difficulties in observing QWS's in Au films, or it could be due to problems encountered when analyzing such data because of strong hybridization between *sp* and *d* states and their

overlapping energy regions, which are more pronounced in Au as compared to Ag and Cu. Therefore, in the present work, special emphasis is placed on the proper distinction of QWS's of different character (*sp* and *d*).

The Au-film-thickness region investigated in our work includes submonolayer coverages and thickness values of about 4–5 and 10–15 ML, which according to Refs. 7–11 have to correspond to two oscillation periods for the exchange coupling between ferromagnetic layers if we take the systems Fe/Au(111)/Fe and Co/Au(111)/Co as examples. However, in our work the W(110) surface has been used as substrate for growth of the Au film in order to investigate quantum-well state formation and behavior independently of the influence of ferromagnetic layers. The choice of W(110) was motivated by the smooth character of the surface which allows to grow epitaxial Au(111) films of high quality.[32] In addition, W(110) has a comparatively low density of states in the energy region interesting for the formation of Au-derived QWS's.[33,34] Moreover, W(110) is characterized in the direction perpendicular to the surface (the Γ*N* direction of the bcc Brillouin zone) by an energy gap for any symmetry in a binding-energy region between 6.3 and 3.3 eV. Generally, the existence of a large energy gap provides an enhanced confinement of electrons and the formation of well-developed standing electron waves inside of the adsorbed layer. If one also takes the symmetry of wave functions into account, one realizes that the effective energy gap in the W substrate, which is responsible for electron confinement, has to be extended to the range from 6.3 to 2 eV.[22,28] Our analysis of the behavior of the observed *sp*- and *d*-derived QWS's has been carried out in the framework of the extended phase accumulation model which has successfully been applied to QWS formation in the Ag(111)/W(110) system.[30] In comparison to the conventional phase accumulation model,[4,12,16,31] this extended model[30] includes a phase-shift contribution related to the scattering of electron waves confined in the Au layer at

corresponding substrate states located in the energy region outside of the W(110) energy gap. The comparison with experiment carried out in the present work shows a good correlation between theoretical estimates made on the basis of this model and our experimental results, and permitted us to test assumptions about the assignment to *sp*- and *d*-derived QWS's. For additional confirmation of this assignment, further studies involving a Ag monolayer as interlayer in a Au/Ag/W(110) system have been undertaken. On the one hand, this system is characterized practically by the same dependence of the QWS energies on the total (Au+Ag) overlayer thickness. On the other hand, the intensity of Au *d*-derived QWS's is significantly suppressed in this system. Comparison among those QWS's that form in both Au/W(110) and Au/1-ML-Ag/W(110) allowed us to distinguish QWS's of different character and confirm the validity of the extended phase acculation model for analysis of QWS's formed in ultrathin Au(111) layers. After some experimental details, first the pure Au/W(110) system will be discussed, followed by the system with an extra Ag interlayer. The phase accumulation model will be discussed afterwards, followed by an analysis of angle-dependent spectra.

II. EXPERIMENT

The experiments were carried out with linearly polarized synchrotron radiation at the UE56/2 and U125/1 PGM beamlines[35] of BESSY II using a VG Escalab spherical analyzer with 1° angle resolution in a vacuum chamber with 9×10⁻¹⁰-mbar base pressure. Photoemission spectra were measured with mixed ($s+p$) polarized light in normal-electron-emission geometry unless specifically mentioned. In order to provide high surface sensitivity, a photon energy of $h\nu = 62.5$ eV has been chosen. Prior to film deposition, the W substrate has carefully been cleaned by annealing at 1200 °C in an oxygen atmosphere of 5×10^{-8} mbar and subsequent flashing to 2000–2200 °C. The presence of a sharp $p(1\times1)$ low-energy-electron-diffraction pattern and the absence of O 1s and C 1s photoemission intensities have been verified before overlayer deposition. Thin films of Au (and Ag) have been deposited *in situ* onto the W(110) substrate held at room temperature. Au (and Ag) have been evaporated from small metal pieces melted on W-Re wires which were heated resistively. We observe that the spectral shape changes continuously with thickness. In order to determine the maxima of intensity changes, we measured a large number of spectra (about 15 spectra per ML for low coverages and 6–7 spectra per ML near 15-ML thickness). Thicknesses of Au and Ag overlayers were determined by a calibration of the evaporators with a quartz microbalance just before and after each series of deposition. Deposition rates were in the range $(3-5)\times10^{-3}$ Å/s. It is likely that this small growth rate renders the growth mode in the present experiment close to layer by layer. This has previously been analyzed for the initial stages of Au growth on W(110).[28,32] A good confirmation for this are the intensity changes of quantum-well states that we observe. Quantum-well peaks characteristic of a
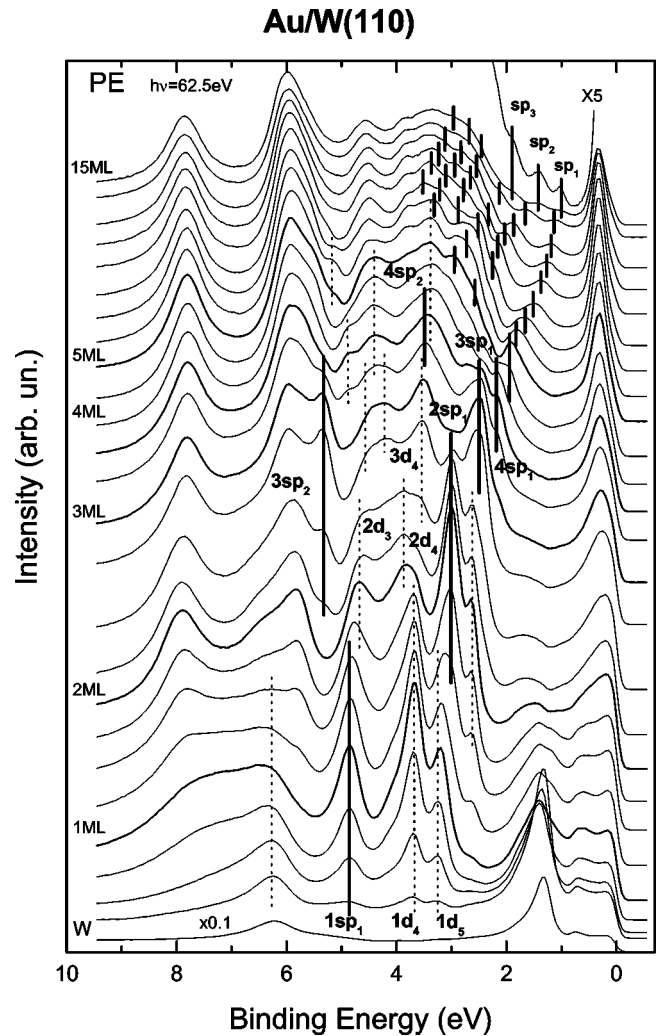
FIG. 1. Series of normal-emission photoelectron spectra of Au/W (110). Pronounced quantum-well-derived peaks appear. For selected peaks, vertical lines mark the assignment to QWS's of *sp* character (thick solid lines) and *d* character (dashes). For further assignments, cf. Fig. 2.

certain number of layers practically disappear before the ones representing the next layer appear (see further below).

III. RESULTS FOR Au/W(110)

In Fig. 1, a series of normal-emission photoelectron spectra of Au/W(110) is shown. The spectra have been selected from a much wider set (about one out of 10–15 spectra). The spectra corresponding to deposition of the first five complete monolayers are displayed as thicker lines and marked by corresponding labels on the left-hand side of the spectra. In the bottom of the figure, the spectrum for the clean W(110) surface is presented in addition. This W spectrum is characterized by a main feature at about 1.2–1.3-eV binding energy (BE) plus weak features at BE's of about 1.8 and 0.7 eV. Deposition of Au leads to a decreasing intensity of the W-derived features and the appearance and growth of Au-derived features located at BE's of about 6.2, 4.85, 3.8, and 3.3 eV. The main features, with BE's of 4.85 and 3.8 eV,

have maximum intensities at coverages corresponding to 1 ML of Au. Beyond 1 ML, their intensities decrease and they practically disappear. Further deposition of Au up to 2 ML is followed by appearance of a pronounced feature at about 3.0-eV BE and a series of weak features of BE's of 4.6, 4.0, and 2.7 eV. A feature at about 8-eV BE appears in the spectra between 1 and 2 ML of Au and does not change its position up to at least 15 ML, which is the largest thickness studied in the present work. The feature at 3.0-eV BE has an intensity maximum at 2-ML thickness. Beyond 2 ML, it disappears abruptly from the spectra. Deposition of the third Au monolayer is followed by the appearance and growth of a strong feature of 2.5-eV BE which in turn disappears during completion of 4-ML Au thickness. Simultaneously with this, the formation of a feature at 5.5-eV BE can be clearly observed for coverages in the range of 3 ML. As to the other features that are observed in the spectra, deposition of up to 4-ML Au is also characterized by a continuous shift of all of the observed features toward the Fermi level. An increase of the Au thickness up to 4 and 5 ML is followed by the formation of pronounced features of 2.2- and 2.0-eV BE's, respectively.

On the basis of the data presented, we conclude that almost all of the features formed up to 5-ML Au coverage are characterized by abrupt changes of their BE's and by intensity maxima which are reached (as will be seen) just during formation of each new Au monolayer. The positions of the features corresponding to formation of 1, 2, 3, 4, and 5 ML are marked in Fig. 1 by vertical lines—solid and dotted lines are for sp- and d-type states, respectively. The labels for sp states are of the form isp_j, where i denotes the number of deposited monolayers and j the quantum number of the QWS, whereas the labels for d states are of the form id_k with k denoting the symmetry for the parent bulk band, i.e., 1 for Λ_6, 2 for Λ_{4+5}, 3 for Λ_6, 4 for Λ_6, 5 for Λ_{4+5}, and 6 for Λ_6.

At higher Au coverages we can no longer distinguish the steplike changes in BE due to the small energy differences between QWS's of successive layers and the concomitant difficulty to resolve these differences. As a result of this, further Au deposition leads to seemingly continuous shift of the observed features toward lower BE up to the edge of the Au sp band, which corresponds to about 1-eV BE in the $\Gamma(\Lambda)L$ direction. Nevertheless, we can, at least up to 15 ML, observe well-developed structures in the spectral intensity due to sp-band states (at least three peaks at BE's of 1, 1.4, and 1.8 eV). In addition to this, we can distinguish a series of weak features at higher Au coverages which are successively shifted towards lower BE's. These features appear in the energy region of Au d states, i.e., for BE's between 2.2 and 3.5 eV, and shift with increasing thickness up to the edge of the Au d band (i.e., 4.7 eV for d_3, 2.9 eV for d_4, and 2.2 eV for d_5 at the L point).

These energy shifts are summarized both for Au sp- and d-derived features in Fig. 2(a) in a plot of binding energy vs Au deposition time. Here, open circles are for the main features, and crosses are for the weak structure observed in the region of d states. In addition, the deposited Au thickness (in monolayers) is given at the top of Fig. 2(a). Note the sharp steplike character of intensity changes which are presented in Fig. 2(b) for the main features in the spectra noted above. Each feature assumes an intensity maximum when formation of Au monolayer is completed. The notation of the main maxima in Fig. 2(b) corresponds to that presented in Fig. 1. We could distinguish small changes of intensities of some features up to 7–9 ML of Au. From an analysis of the BE behavior presented in Fig. 2(a), we can again see that after deposition of 5-ML Au the energy changes appear to be rather continuous. Still, we can distinguish features that approach the edge of the Au sp valence band from those weak features (marked as crosses) that tend toward the edge of the Au d band.

Superimposed on the experimental results, Fig. 2(a) shows data obtained from the extended-phase-accumulation-model analysis as horizontal bars (for Au sp states) and solid squares and diamonds (for Au d_5 and d_4 states, respectively). These data will be described and discussed in Sec. V.

IV. RESULTS FOR Au/1-ML Ag/W(110)

Figure 3 shows an analogous series of normal-emission spectra of various Au thicknesses deposited onto W(110) precovered with a Ag interlayer of about 1-ML thickness. The spectra corresponding to formation of the first Au monolayers are marked on the left side of the spectra. In the bottom of the figure the spectrum corresponding to the initial system of 1-ML Ag/W(110) is presented. The spectrum is in agreement with the one for 1-ML Ag/W(110) of our previous work.[30] The peaks related to Ag are located around 4–5-eV BE. The W-derived features are situated at BE's between 0.5 and 2 eV. Upon Au deposition the Ag- and W-derived features are weakened, and eventually disappear from the spectra. At 2-ML total (Au+Ag) thickness the spectra are already very similar to those observed for 2-ML Au/W(110). However, now the binding energy of the pronounced feature in the spectrum is about 3.2 eV and the features in the region of 3.5–4-eV binding energy are absent. Before, however, at the initial stages of Au deposition, obviously during completion of a total first monolayer, weak features with BE's of about 4.8 and 3.8 eV can also be observed. Deposition of a third total (Au+Ag) monolayer leads to disappearance of the feature at 3.2-eV BE, and is followed by growth of two new pronounced features located at BE's of about 5.4 and 2.6 eV. Further deposition of Au up to 4- and 5-ML total (Au+Ag) thicknesses is characterized by reduction of the features noted above and growth of features located at BE's of 2.2 and 2.0 eV, respectively. Similarly to the pure Au/W(110) system, upon further Au deposition we can no longer distinguish the steplike changes of BE's. Increasing the thickness of deposited Au, the peaks are rather continuously shifted toward lower BE's up to the edge of the Au sp states. Nevertheless, at thicknesses of about 10–12 ML we can clearly distinguish in the region of Au sp states, i.e., above the Au d band edge, two well-developed peaks which can be described as QWS's of sp character. Besides this, at higher Au coverages a series of weak features can be distinguished [similar to the case of Au/W(110)] with BE's located within the energy range of the Au d valence band. Two diagrams show the changes of energy positions upon Au deposition
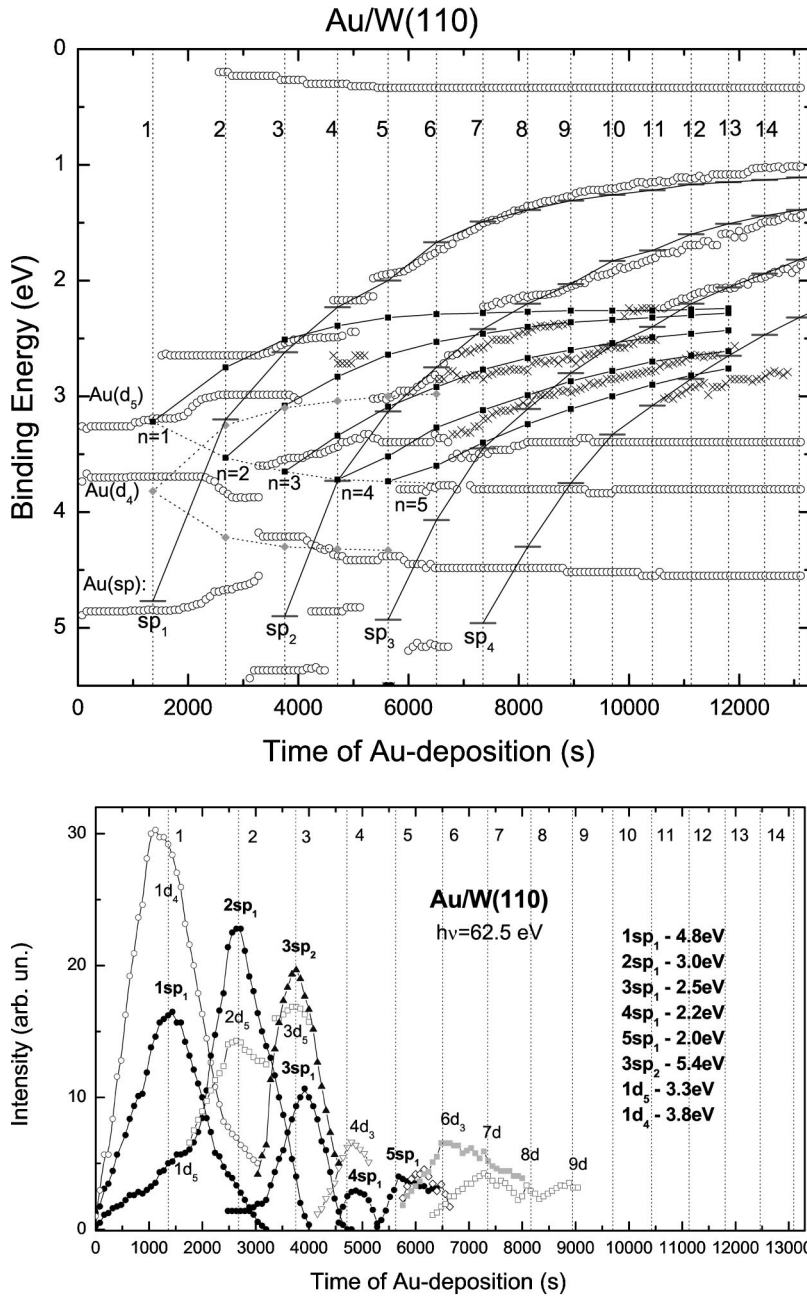
FIG. 2. (a) Binding energies of quantum-well states as a function of deposition time. In addition, the coverage (in ML) is given at the top. Open circles are for main features, and crosses are for the weak structures observed in the region of d states. (b) Intensities of main features vs deposition time and coverage. Maxima appear when growth of an integral number of layers is accomplished. The solid and dotted lines simply connect theoretical values for sp and d quantum-well states characteristic of each additional Au monolayer.

[Fig. 4(a)] and the corresponding intensity changes of the main features [Fig. 4(b)]. The total thickness of the overlayer (Au+1 ML Ag) is given (in ML) in the upper parts of the figures. As in Fig. 1, open circles mark main features, crosses mark the series of weak features in the Au d energy range, and the notation also corresponds to the one used in Fig. 1.

In Fig. 4(a), we can clearly distinguish the steplike character of the BE changes in the initial stage of Au deposition. Moreover, analyzing the variations of their intensities we can easily identify the completion of each new monolayer from the maxima of the corresponding photoemission features in the same way as has been done for the Au/W(110) system. Note, however, that Au/Ag/W(110) (see Fig. 3) is, in contrast to Au/W(110) (see Fig. 1), characterized by the absence of several peaks at the initial stage of Au deposition. These are features that appear in the region of the Au d band and which

we will ascribe (in the discussion below) to formation of Au d-derived QWS's. In other words, in the case of the Au/Ag/W(110) system, in the initial stage of Au deposition practically only QWS's of Au sp character are observed.

In Fig. 4(a), for comparison, the data obtained on the basis of the extended-phase-accumulation-model analysis are also shown by horizontal bars and solid squares and diamonds. These data will be described and discussed below.

V. EXTENDED PHASE ACCUMULATION MODEL

The observations made for both systems Au/W(110) and Au/1-ML-Ag/W(110), i.e., that normal-emission photoelectron spectra show: (i) a number of pronounced features at the initial stages of growth, the BE's of which change in a step-
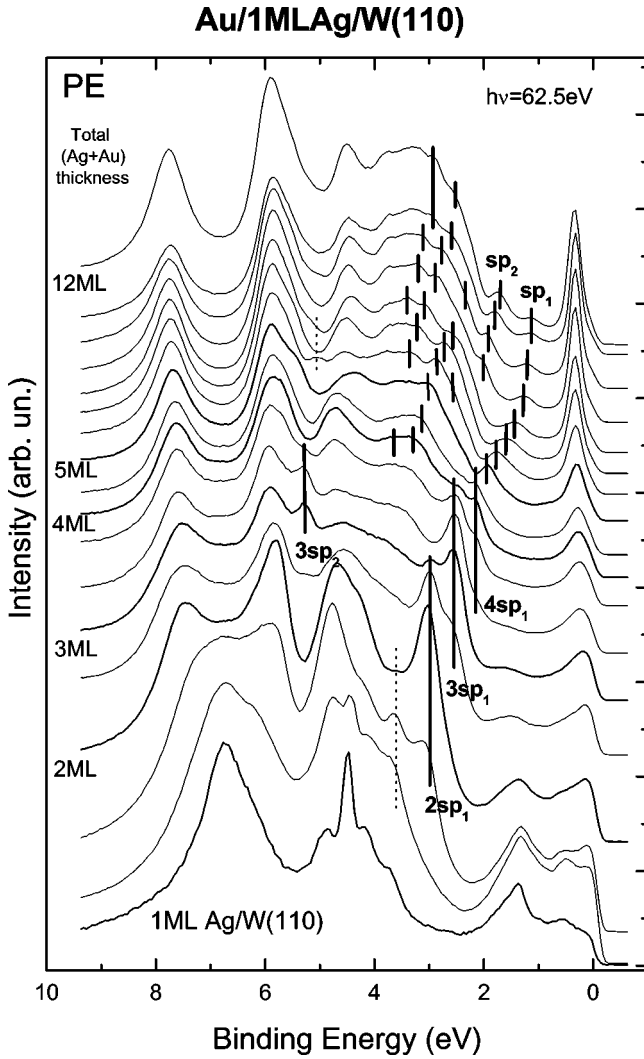
FIG. 3. Same as Fig. 1 for Au on W(110) precovered with a monolayer-thick Ag interlayer. Quantum-well states of *sp* type develop throughout the Au/Ag overlayer, and are almost indistinguishable from Fig. 1, whereas formation of Au *d*-type quantum-well states is inhibited at low coverages.

like way, (ii) a series of periodically arranged features for Au coverages from 5–6 ML up to high Au coverages (at least 15 ML), and (iii) continuous shift with thickness towards the edges of Au *sp* and Au *d* bands, are similar to those from classical QWS's formed on various substrates,[1,2,4,12–30] and consequently one expects that they also can be interpreted in the framework of corresponding QWS models. However, in contrast to classical cases of QWS's, which typically form inside of an energy gap of the substrate electronic structure, for the systems investigated in the present work the energies where QWS's are observed largely cover the energy region outside of the W(110) energy gap. For comparison, see the corresponding valence-band electronic structures along the surface normal for Au(111) and W(110) in Fig. 5(a) shown in the ΓL and ΓN directions, taken from Refs. 36 and 37, and Refs. 33 and 34, respectively. There are two consequences for the analysis of the present data that are readily apparent from Fig. 5(a): First, in the energy region outside of the

substrate gap, standing electron waves which are responsible for formation of QWS's are not fully confined. These effects are so large that we already have to account for a modification of the phase shift upon partial reflection at the interface due to the influence of the substrate electronic structure.[30] Second, in comparison to classical QWS's, the ones formed in the present systems are characterized by significant degeneracy of Au *sp* and Au *d* states. This holds especially for the initial stage of Au deposition, when both kinds of states have to be situated in exactly the same energy region.

For analysis and interpretation of the observed QWS's we used the extended phase accumulation model, which was first described in Ref. 30, and was successfully applied to QWS's formed in the system Ag/W(110). The main equation of the extended phase accumulation model consists of the one used in the conventional phase accumulation model[12,31] plus an additional term Φ_{scatt} responsible for the phase-shift changes related to scattering at substrate states outside of the substrate energy gap. In this case, the equation acquires the form

$$\Phi_B + \Phi_C + 2kd - \Phi_{\text{scatt}} = 2\pi n, \qquad (1)$$

where Φ_B and Φ_C are the phase shifts related to reflection at the surface barrier and at the interface, respectively, and k is the wave vector of an electron propagating in an overlayer of thickness d. Expressions for Φ_B and Φ_C are usually taken from Refs. 12 and 31

$$\Phi_B/\pi = [3.4 \text{ eV}/(E_V^* - E)]^{1/2} - 1, \qquad (2)$$

where E_V^* is the vacuum level and E the electron energy measured from the bottom of the inner potential. With E_U and E_L denoting the upper and lower edges of the substrate energy gap, respectively, Φ_C is expressed as

$$\Phi_C = 2 \arcsin[(E - E_L)/(E_U - E_L)]^{1/2} - \pi. \qquad (3)$$

For the term $2kd$ we use the formula

$$2kd = 2ka_0 N = 2 \arccos\left(1 - \frac{2E}{E_U^* - E_L^*}\right) N, \qquad (4)$$

with E_U^* and E_L^* for upper and lower band edges of the overlayer, a_0 for the thickness of one adsorbed monolayer, and N for the number of adsorbed monolayers. This expression has been obtained on the basis of the formula used in the tight-binding-model for the simplest linear chain approximation[38,39]

$$E = -0.5(E_U^* - E_L^*)(1 + \cos kd), \qquad (5)$$

which can be well applied in the monolayer limit of overlayer thickness.

The dependencies of the terms Φ_B, Φ_C, and $2ka_0 N$ characteristic of the Au *sp* state and two upper Au *d* states are displayed in Fig. 5(b) for the first and second Au monolayers.[40] Here also the main energy parameters are presented for the Au and W valence bands along [111] and [110], respectively, i.e., the values for valence band edges
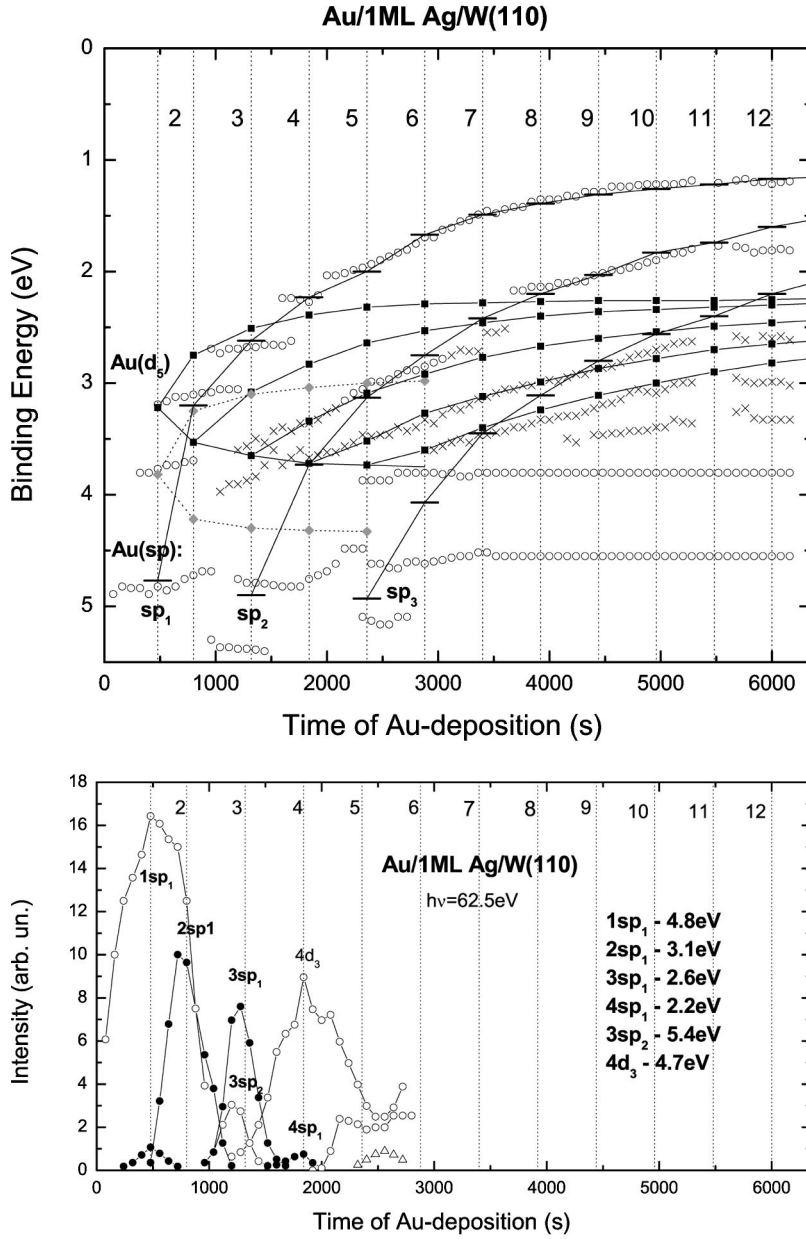
FIG. 4. Same as Fig. 2 for the system with the extra Ag interlayer.

and the vacuum level. These values are taken from Refs. 36, 37, 41, and 42 for Au and Refs. 33 and 34 for W.

VI. APPLICATION TO EXPERIMENTAL DATA

As we can see, the W(110) valence-band structure in the region of QWS formation, has an energy gap of Σ_5^1 states between 6.3- and 2.0-eV. BE's (superscripts and subscripts denote single- and double-group symmetries, respectively). As Σ_5^2-symmetry states appear between 3.3 and 1.2 eV, an absolute Σ gap opens between 6.3 and 3.3 eV. In this energy range, electrons are fully confined to the Au overlayer. On the other hand, as symmetry rules state that Au *sp* QWS's can couple only to Σ_5^1 substrate states[27,28] (we assume that single-group properties prevail), the electron waves formed in the Au overlayer in the energy region of 3.3–2.0 eV can also be reflected at the interface with W, but with an addi-

tional phase shift related to partial scattering at Σ_5^2 states.[30] In Fig. 5(b), the experimental phase-shift changes across this energy range are shown by open circles. This phase shift has been determined experimentally on the basis of observed BE's of *sp* QWS's [see Eq. (3) of Ref. 28].

First of all, we can see that in the binding-energy region between 3.3 and 1.2 eV this experimental phase shift differs from the phase shift of the conventional phase accumulation model ($\Phi_B + \Phi_C - 2\pi n$). This is just the region of Σ_5^2 states (see the dash-dotted lines in this region). We found that the experimental phase shift can best be approximated by the following choices of Φ_{scatt}: (i) Zero in the range of the absolute Σ gap (Σ_5^1 and Σ_5^2 gap, i.e., 6.3-3.3-eV BE), i.e., in this region the total phase shift can be described on the basis of just Φ_B and Φ_C. (ii) An expression according to Eq. (4) [with $N=1$; see the dashed curve from 3.3 to 1.2 eV in Fig.

(a)

(b)
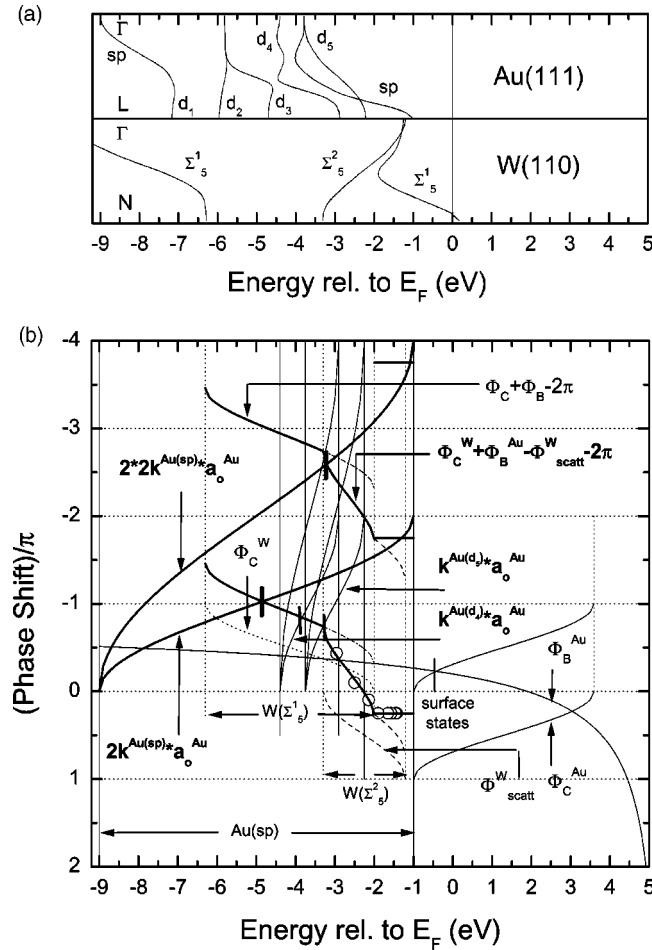
FIG. 5. (a) Bulk band structures of Au(111) and W(110) taken from Refs. 36 and 37 and 33 and 34, respectively. The presentation is such that the vertical direction in the figure is normal to the film plane. (b) Phase accumulation model for the first two monolayers $N=1$ and 2. Open circles are experimentally determined values for the phase shift. As an example for the graphical solution of Eq. (1), only selected intersections of the phases accumulated under propagation and due to scattering are marked.

5(b)] in the Σ_5^2 range inside the region of the Σ_5^1 gap (3.3–2.0-eV BE). (iii) A simple constant dependence in the region of both Σ_5^1 and Σ_5^2 states (2−1.2–eV BE).[40] The resulting energy dependence of $\Phi_B+\Phi_C-\Phi_{scatt}-2\pi n$ is shown in Fig. 5(b) by broken lines for $n=0$ and $n=1$ (i.e., shifted upward by 2π). The contributions of the phases accumulated under propagation through the adsorbed layer $2kd=2ka_0N$ is also given for $N=1$ and 2 for the Au *sp* band and two upper Au *d* bands. The intersections between the curves mentioned have been marked by thick vertical ticks. These are the graphical solutions of Eq. (1), and determine the BE's of corresponding QWS's. In Fig. 6, the same curves are presented for up to about $N=7$ ML. Also, the energy scale has been zoomed so that the phases $2kd$ can easier be distinguished for *sp* (solid lines), d_4 (thin solid lines), and d_5 (dashed lines). The vertical ticks marking the intersections are thick for Au *sp* states and thin for Au *d* states. These are also the energies that have been introduced into Figs. 2(a) and 4(a) for comparison with the experimental results (hori-
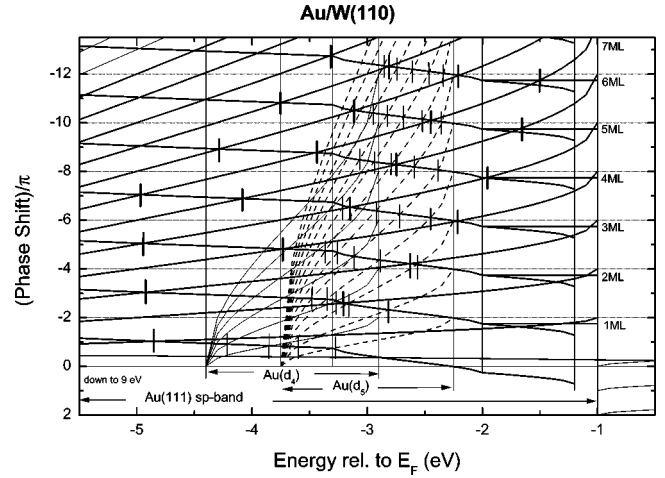
FIG. 6. Same as Fig. 5(b) for larger thicknesses up to $N=7$ ML. Phases $2kd$ have been marked for *sp* (solid lines), d_4 (thin solid lines), and d_5 (dashed lines). The vertical ticks marking the intersections are thick for Au *sp* states and thin for Au *d* states.

zontal bars for Au *sp* states, solid squares for Au d_5 states, and solid diamonds for Au d_4 states).

It becomes apparent from this comparison (in Figs. 2 and 4) that good agreement is reached for both systems Au/W(110) and Au/1-ML-Ag/W(110) and all Au coverages investigated. Not only are Au *sp*-derived states well described but also QWS's corresponding to the upper Au *d* bands. This fact is important, since it permits us to unambiguously assign QW peaks to their orbital character (*sp* and *d*). For example, the intense peak at a comparatively high BE of 4.8 eV that appears for 1-ML Au can be assigned to an *sp*-type QWS, whereas features at lower BE's, e.g., at 3.3 and 3.8 eV, are assigned to d_5 and d_4 QWS's of the Au monolayer, respectively.

Increase of the Au layer thickness up to 2, 3, 4, and 5 ML corresponds to the formation of QWS's of Au *sp* character with BE's of 3.0, 2.5–2.6, 2.15, and 2.0 eV, respectively. These features reach maximum intensities right at these integer thicknesses. For Au/1-ML-Ag/W(110), the QWS's appear practically at the same BE's. Only for 2 and 3 ML of Au for the Au/Ag/W system, the corresponding BE's have slightly higher values (3.2 and 2.7 eV). Generally, the differences of BE's of *sp*-type QWS's between the two systems vanish with increasing Au thickness.

Besides the main Au *sp* QWS's with $n=1$, branches with $n=2$ and 3 can also be well distinguished. For the energy region outside of the Au *d* band, i.e., for BE's lower than 2.2 eV, the three branches of the Au *sp*-derived QWS's states are nicely visible. These branches are marked in Figs. 2(a) and 4(a) as sp_1, sp_2, and sp_3, and are well described by extended phase accumulation models both for Au/W(110) and Au/1-ML-Ag/W(110) systems. Branches with higher values of n have not been observed, probably due to the limited overlayer thickness of about 15 ML and, as a consequence, their overlap with Au *d* states.

The extended phase accumulation model assigns the series of weak features with BE's beyond 2.2 eV [crosses in Figs. 2(a) and 4(a)] to Au d_5 QWS's with $n=1$, 2, 3, 4, and

5. These states correspond to upper Au d_5 states located in the energy region between 2.2 and 3.8 eV. Predicted BE's for Au d_5 QWS's from our model are shown in Figs. 2(a) and 4(a) by solid squares, and are marked by the quantum numbers $n = 1$, 2, 3, 4, and 5. There are some photoemission features which can be described as Au d_4-derived QWS's, among these the 3.8-eV feature for 1-ML Au. We present extremal BE changes of Au d_4-derived QWS's, i.e., BE's of the corresponding main features, by solid diamonds in Figs. 2(a) and 4(a).

Note that the observation of several branches of d-derived QWS's is an important experimental result. To our knowledge this is practically the first time d-derived QWS's are properly accounted for. In an early work on the same system, Au/W(110), a number of peaks were observed in Au/W(110) up to 8-ML thickness; however, they have been assigned to sp states.[28] In the present work we can clearly distinguish the asymptotic behaviors of Au sp states (a trend toward the edge of the sp band at 1-eV BE) from the ones of Au d_5 states (trend toward 2.2 eV). In fact, almost all of the peaks reported in Ref. 28 are now assigned to d-type QWS's via Figs. 5 and 6.

There is another observation from the comparison of the systems Au/W(110) and Au/1-ML-Ag/W(110): in the latter the intensity of d-type QWS's is substantially lower, especially in the first stages of Au deposition. See, e.g., the spectra for 2-ML total (Au+Ag) thickness in Fig. 3: the features with BE's between 3.5 and 4.5 eV and the feature with 2.7-eV BE are practically absent. However, for sp QWS's we observe well-pronounced peaks (see $2sp_1$, $3sp_1$, etc.). Since sp-derived quantum-well states appear to be well developed in both systems (as do d-derived quantum-well states for larger thickness), it appears likely that differences in the electronic structure, e.g., between the energies of Au d and Ag d states, cause this behavior. In view of the similarity of Au $6sp$ and Ag $5sp$ wave functions and energy ranges, the formation of common QWS's characterized by a total (Au+Ag) thickness can be expected, and such common quantum-well states have been observed for Cu and Ni $4sp$ states.[43] *The present work indicates that in the same system where formation of sp-type* QWS's *occurs throughout the* Au+Ag *film, the formation of standing waves of mixed* Au d *and* Ag d *character is inhibited.*

VII. DISPERSION WITH $\mathbf{k}_\parallel$

For an experimental analysis of the nature of the observed QWS's we carried out additional measurements of the dispersion with the electron emission angle, i.e., $\mathbf{k}_\parallel$, along the $[1\bar{1}0]$ direction. We studied several thicknesses, and the results are displayed in Fig. 7 for Au/W(110) (thicknesses of 1, 2.5, and 3.5 ML) and in Fig. 8 for Au/1-ML-Ag/W(110) (total thicknesses of 2, 3, and 8 ML).

First, we want to discuss the assignment of sp and d states. We see, e.g., for 3.5-ML Au/W(110), a strong parabolic behavior of the $3sp_1$ state at 2.5-eV BE, whereas the $3d_5$ state at the same thickness and BE shows a very flat dispersion. At higher BE, d-type QWS's are even characterized by a dispersion toward higher BE's [see $1d_4$ and $1d_5$

QWS's for Au/W(110)]. Such a dispersion to higher BE with increasing emission angle was already noted for d states of noble metals [for Cu/Co(100), see Ref. 43]. Together with our finding of dispersion to lower BE's of the $1sp_1$ and $3sp_2$ peaks, characteristic of sp QWS's, a dispersion to higher BE can be taken as further indication for d character of the QWS's in the present systems.

We readily see that for thicker overlayers [3.5 ML for Au/W(110) and 3 and 8 ML for Au/1-ML-Ag/W(110)], where sp-derived QWS's, appear outside of the Au d band, i.e., at BE's lower than 2.2 eV, these sp-type QWS's show a pronounced angle dispersion toward lower BE's. In addition, thick overlayers display the dispersion of the surface states of Au(111). This behavior typical of sp-type QWS's was measured for a number of Ag and Cu QW systems,[14,16,19,20,42,44,45] and in some cases the dispersion was followed for large off-normal angles where it turns back to higher BE's.[20,43] This behavior has been assigned to hybridization between QWS's and substrate-derived states.[20,43] In our data, we have a large number of states and thicknesses, and can therefore discuss the QWS dispersion depending on thickness and energy range of QWS's.

As for Au sp-type QWS's, we observe a flattening of dispersion with increasing BE's. This is not typical of classical QWS's (see, e.g., Refs. 14, 16, and 19). The change in dispersion of QWS's around $\bar{\Gamma}$ is usually described[19,20,42,44,45] with an increased effective mass m^*, and assigned to enhanced hybridization with more strongly localized states of the substrate for thinner films.[44]

On the basis of the present data, the increase of the effective mass can be connected to the hybridization between Au sp and Au d states, which is expected to increase when sp-derived QWS's are located in the region of the Au d band, that is here for low Au coverages. In more detail, we see that at 3 ML (Fig. 7), the $3sp_1$ state at the upper edge and almost outside of the Au d band disperses much more strongly than the $3sp_2$ state, which is completely degenerate with Au d states. Moreover, the dispersion of the $8sp_3$ state (Fig. 8) is not very different from the one of the $3sp_1$ state at the same binding energy, but has a weaker dispersion than the $8sp_2$ state further up in energy. *Basically, all states outside of the Au* d *range have a much smaller effective mass than the ones inside.*

VIII. CONCLUSION

On the basis of our experimental data, and from our analysis using the extended phase accumulation model, we arrive at the following conclusions.

(1) Deposition of thin layers of Au onto the W(110) surface, with and without a monolayer-thick Ag interlayer, leads, in normal-emission photoelectron spectra, to the occurrence of a series of distinct peaks in the energy region of Au sp and Au d bands. These can be described as QWS's, which shift toward lower BE's with increasing Au thickness. At the initial states of deposition (4–5 ML of Au), BE's abruptly change, indicating the formation and completion of individual Au monolayers. For larger thicknesses (beyond
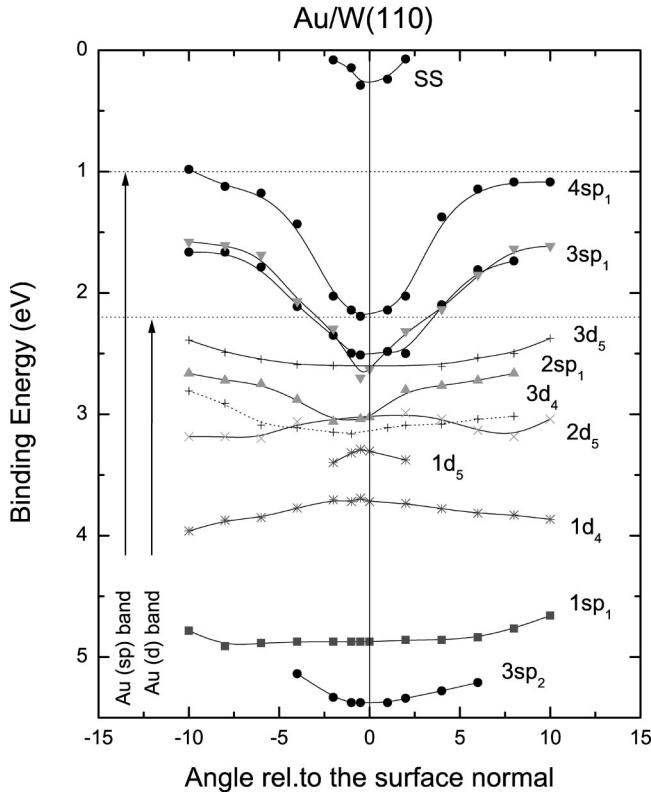
FIG. 7. Angle dispersion of quantum-well states derived from photoemission spectra of Au/W(110) for thicknesses of 1, 2.5, and 3.5 ML. Quantum-well states of *d* character can be identified by their flat dispersion. In addition, the influence of *sp-d* hybridization inside the Au film influences the dispersion of *sp*-type quantum-well states.

5–6 ML), the behavior with thickness resembles a continuous shift. This shift approaches the lower band edges of the Au *sp* and Au *d* bands, respectively.

(2) QWS's in both systems, Au/W(110) and Au/1-ML-Ag/W(110), are characterized by approximately the same BE values, provided one characterizes the states by a total (Au+Ag) layer thickness.

(3) Detailed analysis shows that energy positions and their behavior with thickness can be well described in the framework of the extended phase accumulation model. The model requires a consideration of the phase shift caused by a partial scattering of electrons at substrate bulk states, in the present case these are W Σ_5^2 states in the energy region of the Au *sp*- and Au *d*-derived QWS's. The agreement reached in this way is good for both systems investigated.

(4) Our model analysis is essential for the assignment of the large number of peaks observed. We distinguish three
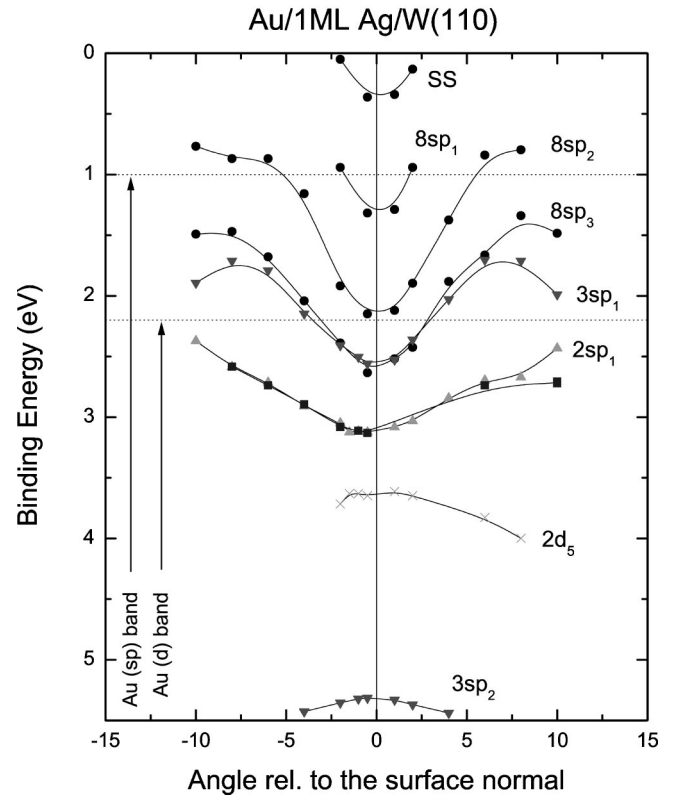
FIG. 8. Same as Fig. 7 for the system with Ag interlayer. The total thicknesses studied were 2, 3, and 8 ML.

branches (i.e., states for $n = 1$, 2, and 3) of Au sp_n-derived QWS's and $4-5$ branches of Au d_5-derived QWS's. For 1–2-ML Au, we also observe Au d_4-derived QWS's.

(5) Analysis of dispersion with $\mathbf{k}_{\parallel}$ around $\bar{\Gamma}$ shows a pronounced parabolic behavior toward lower BE for the Au *sp*-derived QWS's, and dispersion toward higher BE's for Au *d*-derived QWS's. This conclusion, applied to the observed QWS's, confirms their assignment based on an extended phase accumulation model. Moreover, the effective mass of QWS's is rather determined by *sp-d* hybridization within the overlayer than at the interface.

[1] P Grünberg, R. Schreiber, Y. Pang, M. B. Brodsky, and H. Sowers, Phys. Rev. Lett. **57**, 2442 (1986).

[2] M. N. Baibich, J. M. Broto, A. Fert, F. Nguyen Van Dan, F. Petroff, P. Etienne, G. Creuzet, A. Friederich, and J. Chazolas, Phys. Rev. Lett. **61**, 2472 (1988).

[3] S. S. P. Parkin, N. More, and K. P. Roche, Phys. Rev. Lett. **64**, 2304 (1990).

[4] J. E. Ortega and F. J. Himpsel, Phys. Rev. Lett. **69**, 844 (1992); F. J. Himpsel, J. E. Ortega, G. J. Mankey, and R. F. Willis, Adv. Phys. **47**, 511 (1998); J. E. Ortega, F. J. Himpsel, G. J. Mankey,

and R. F. Willis, Phys. Rev. B **47**, 1540 (1993).

[5] K. Garrison, Y. Chang, and P. D. Johnson, Phys. Rev. Lett. **71**, 2801 (1993).

[6] C. Carbone, E. Vescovo, O. Rader, W. Gudat, and W. Eberhardt, Phys. Rev. Lett. **71**, 2805 (1993).

[7] P. Bruno and C. Chappert, Phys. Rev. Lett. **67**, 1602 (1991).

[8] V. Grolier, D. Renard, D. Bartenlian, P. Beauvillian, C. Chappert, C. Dupas, J. Ferre, M. Galtier, E. Kolb, M. Mulloy, J. P. Renard, and P. Veillet, Phys. Rev. Lett. **71**, 3023 (1993).

[9] J. J. de Vries, W. J. M. de Jonge, M. J. Johnson, J. van de Stegge, and A. Reinders, J. Appl. Phys. **75**, 6440 (1994).

[10] S. S. P. Parkin, R. F. C. Farrow, R. F. Marks, A. Cebollada, G. R. Harp, and R. J. Savoy, Phys. Rev. Lett. **72**, 3718 (1994).

[11] K. Koike, T. Furukawa, and Y. Murayama, Phys. Rev. B **51**, 10 260 (1995).

[12] N. V. Smith, N. B. Brookes, Y. Chang, and P. D. Johnson, Phys. Rev. B **49**, 332 (1994).

[13] T. Miller, A. Samsavar, G. E. Franklin, and T.-C. Chiang, Phys. Rev. Lett. **61**, 1404 (1988).

[14] M. A. Mueller, T. Miller, and T.-C. Chiang, Phys. Rev. B **41**, 5214 (1990).

[15] J. J. Paggel, T. Miller, and T.-C. Chiang, Science **283**, 1709 (1999).

[16] T.-C. Chiang, Surf. Sci. Rep. **39**, 181 (2000).

[17] G. Neuhold and K. Horn, Phys. Rev. Lett. **78**, 1327 (1997).

[18] C. Carbone, E. Vescovo, R. Kläsges, D. D. Sarma, and W. Eberhardt, Solid State Commun. **100**, 749 (1996).

[19] C. Carbone, E. Vescovo, R. Kläsges, W. Eberhardt, O. Rader, and W. Gudat, J. Appl. Phys. **76**, 6966 (1994).

[20] T. Valla, P. Pervan, M. Milun, A. B. Hayden, and D. P. Woodruff, Phys. Rev. B **54**, 11 786 (1996).

[21] M. Milun, P. Pervan, B. Gumhalter, and D. P. Woodruff, Phys. Rev. B **59**, 5170 (1999).

[22] J. Feydt, A. Elbe, H. Engelhard, G. Meister, and A. Goldmann, Surf. Sci. **452**, 33 (2000).

[23] K. Garrison, Y. Chang, and P. D. Johnson, Phys. Rev. Lett. **71**, 2801 (1993).

[24] D.-A. Luh, J. J. Paggel, T. Miller, and T.-C. Chiang, Phys. Rev. Lett. **84**, 3410 (2000).

[25] A. Tanaka, H. Sasaki, K. Takahashi, W. Goudo, S. Suzuki, and S. Sato, J. Phys. Chem. Solids **60**, 1995 (1999).

[26] A. Mugarza, J. E. Ortega, A. Mascaraque, E. G. Michel, K. N. Altmann, and F. J. Himpsel, Phys. Rev. B **62**, 12 672 (2000).

[27] D. Hartmann, W. Weber, A. Rampe, S. Popovic, and G. Güntherodt, Phys. Rev. B **48**, 16 837 (1993).

[28] H. Knoppe and E. Bauer, Phys. Rev. B **48**, 5621 (1993).

[29] A. M. Shikin, D. V. Vyalikh, Yu. S. Dedkov, G. V. Prudnikova, V.

K. Adamchuk, E. Weschke, and G. Kaindl, Phys. Rev. B **62**, R2303 (2000).

[30] A. M. Shikin, D. V. Vyalikh, G. V. Prudnikova, and V. K. Adamchuk, Surf. Sci. **487**, 135 (2001).

[31] N. V. Smith, Phys. Rev. B **32**, 3549 (1985).

[32] E. Bauer, H. Poppa, G. Todd, and P. R. Davis, J. Appl. Phys. **48**, 3773 (1977).

[33] R. H. Gaylord and S. D. Kevan, Phys. Rev. B **36**, 9337 (1987).

[34] J. Feydt, A. Elbe, H. Engelhard, G. Meister, Ch. Jung, and A. Goldmann, Phys. Rev. B **58**, 14 007 (1998).

[35] R. Follath, F. Senf, and W. Gudat, J. Synchrotron Radiat. **5**, 769 (1998); K. J. S. Sawhney, F. Senf, M. Scheer, F. Schäfers, J. Bahrdt, A. Gaupp, and W. Gudat, Nucl. Instrum. Methods Phys. Res. A **390**, 395 (1997); M. R. Weiss, K. J. S. Sawhney, R. Follath, H.-Ch. Mertins, F. Schäfers, W. Frentrup, A. Gaupp, M. Scheer, J. Bahrdt, F. Senf, and W. Gudat, in *Synchrotron Radiation Instrumentation*, edited by P. Pianetta, J. Arthur, and S. Brennan, AIP Conf. Proc. No. 521 (AIP, Melville, NY, 2000).

[36] H. Eckardt, L. Fritsche, and J. Noffke, J. Phys. F: Met. Phys. **14**, 97 (1984).

[37] R. Courths, H.-G. Zimmer, A. Goldmann, and H. Saalfeld, Phys. Rev. B **34**, 3577 (1986).

[38] M. Grüne, J. Peltzer, K. Wandelt, and I. J. Steinberger, J. Electron Spectrosc. Relat. Phenom. **98-99**, 121 (1999).

[39] J. Henk and B. Johanson, J. Electron Spectrosc. Relat. Phenom. **105**, 187 (1999).

[40] The experimental phase shift observed here is similar to the one for Ag/W(110) (Ref. 30). As in this energy region the coupling of Au QWS's to $W \Sigma_5^1$ states is possible, reflection and confinement of electrons can only be brought about by differences in the crystalline parameters and atomic number of elements that constitute overlayer and substrate. This possibility was noted in Refs. 16 and 42 in connection with quantum-well resonances in the system Ag/Ni(111). In the strict sense, all of the QWS's reported here, which are outside of the absolute Σ_5^1 gap have to be considered as quantum-well resonances.

[41] R. Piniago, R. Matzdorf, G. Meister, and A. Goldmann, Surf. Sci. **336**, 113 (1995).

[42] T. Miller, A. Samsavar, and T.-C. Chiang, Phys. Rev. B **50**, 17 686 (1994).

[43] P. D. Johnson, K. Garrison, Q. Dong, N. V. Smith, D. Li, J. Mattson, J. Pearson, and S. D. Bader, Phys. Rev. B **50**, 8954 (1994).

[44] H. Sasaki, A. Tanaka, K. Takahashi, W. Gondo, S. Suzuki, and S. Sato, Appl. Surf. Sci. **169−170**, 496 (2001).

[45] F. J. Himpsel and O. Rader, Appl. Phys. Lett. **67**, 1151 (1995).